Chapter 5

Driving stability in side winds

Hans-Joachim Emmelmann

5.1 Introduction

When driving on the open road, the air 'flows over' the vehicle. This causes forces and moments along or about all axes, which affect the driving characteristics. Of these, aerodynamic drag has always attracted most interest.

The components in the other five degrees of freedom greatly influence the lateral dynamic characteristics of the vehicle. Lift and pitching moment occur along with the drag during motion of a vehicle through still air, whereas in side-wind conditions the additional components of side force and yawing and rolling moments develop (see Figs 2.14 and 4.111).

The resultant air forces and moments must be balanced by the reaction forces between the vehicle and the road, gripping through the tyres. The resulting tyre slip angles lead to a deviation from the required direction of travel which must be compensated for by the driver via the steering.

The above phenomenon, which is often referred to as side-wind sensitivity, must be considered from two different aspects. The driver is inconvenienced when continual compensation at the steering wheel is necessary to correct side-wind effects. This leads to stress, premature tiredness and increased risk.

When strong side winds occur from random directions a safety problem can rapidly arise. If the driver lacks the necessary skill or experience to correct for side wind, undesirable deviations from the required vehicle path result and incorrect reaction can lead to loss of control.

If a vehicle is to have good driving characteristics, both aspects of side-wind sensitivity must be considered during the design stage. What follows shows how this is achieved with the help of a general computer model, which establishes the main parameters and presents them as a simple equation. Emphasis is placed on illustrating the methods used rather than the establishment of quantitative results.

5.2 The origin of the forces and moments on a vehicle

5.2.1 Natural wind

The strength and direction of the wind is continuously measured and recorded at a number of geographical locations and at various heights

above the ground, such as 10 to 15 metres. When time-averaged, this airflow profile reveals a normally turbulent boundary layer.

Close to the ground, the fluctuation of wind speed u' is approximately equal to the average value of the speed, i.e. the turbulence level is

$$Tu = \frac{\overline{u'^2}}{V} \approx 1$$

Depending on the condition ('roughness') of the ground, the wind speed at, for instance, half vehicle height, differs from that at a weather station, being either faster or slower. An impression of the form of the boundary layer is shown in Fig. 5.1, from Davenport.[5.1]

In comparison to vehicle height, the boundary layer can be seen to be extremely thick. At vehicle level the wind speed gradient is especially

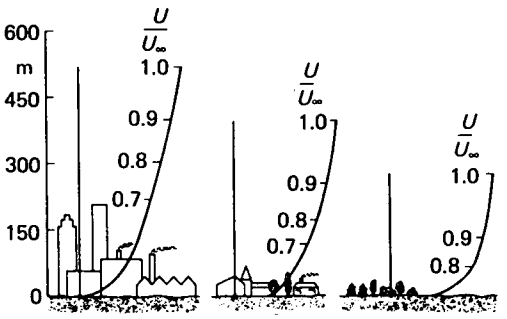

Figure 5.1 Natural wind boundary layers over various ground profiles, after ref. 5.1

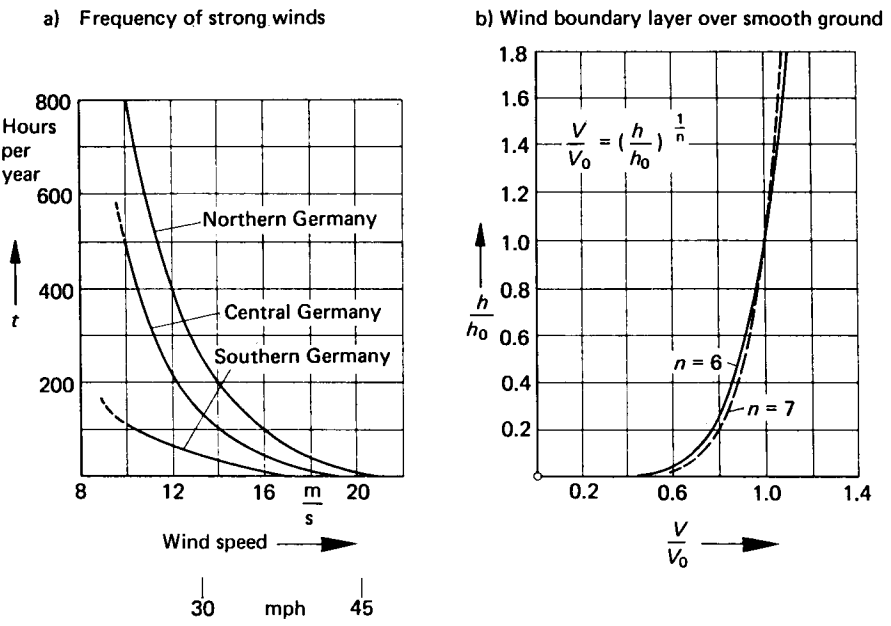

Figure 5.2 Frequency of strong winds in various regions of Germany, and wind boundary layers over smooth ground, after ref. 5.2

steep. Over smooth ground Bitzl[5.2] has shown (Fig. 5.2) that the boundary layer follows a potential function law. Fig. 5.2 also gives data on the frequency of occurrence of strong winds in Germany. Information about side winds—both artificial and natural—has been presented by Karrenberg.[5.3] Some relevant wind speed measurements have been presented by Smith.[5.4] A typical compass card, showing details of wind speed and directions, is shown in Fig. 8.12.

5.2.2 Wind forces due to steady side winds

A special case of side wind consists of a steady airflow which has a constant velocity profile regardless of height. Although hardly possible in nature, this case is in fact provided in the wind tunnel with the exclusion of a thin ground-floor boundary layer (Fig. 5.3). Under natural side-wind conditions, the relationship shown in the right-hand figure is present, whereby

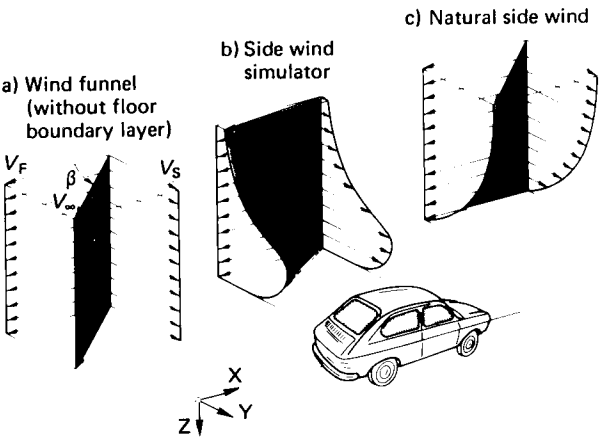

Figure 5.3 Comparison of various side-wind profiles, after Hucho

the whole side-wind profile has boundary layer characteristics. When combined with vehicle speed the resultant air flow profile is strongly twisted. For comparison, the centre part of Fig. 5.3 shows the wind profile of a side-wind simulator, where it can be seen to be seriously distorted. The possibility of simulating side wind using such simulation apparatus is reported in section 12.4.2.

Aerodynamic side force results from the difference in pressure between the windward side and the leeward side of a vehicle. The right-hand side of Fig. 5.4 (after Barth[5.5] and Squire[5.6]) shows the pressure distribution around a horizontal section of a vehicle. On the leeward side considerable negative pressure develops due to high airflow speeds over the vehicle's leading edge. On the windward side, except for a slight negative pressure at the leading edge, a slight positive pressure exists along the vehicle's side to the midpoint. On the rear half of the vehicle, steadily increasing negative pressure is observed. Comparison of the vehicle pressure distribution and that on a wing section shows good correlation, at least in principle. The angle of attack of the wing section was chosen so that the

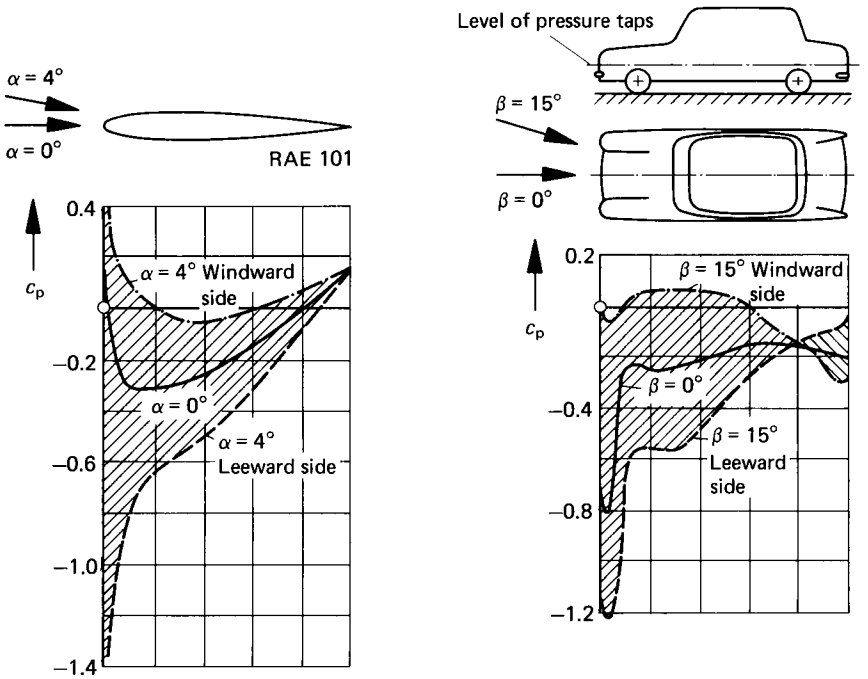

Figure 5.4 Comparison of the pressure distribution around a wing section and a vehicle horizontal section, after refs 5.5 and 5.6

pressure level obtained was approximately similar to that on the vehicle. The pressures of the windward and leeward sides lead to a side force on the vehicle which is directed to the leeward side, and to a yawing moment which generally tends to turn the vehicle's nose to the leeward side.

5.2.3 Aerodynamic stability

The concentration of the negative pressures on the leeward side, at the front of the vehicle, is largely responsible for the aerodynamic yawing moment. This is the characteristic that causes instability. In other words, when side winds on a vehicle cause an angular deviation β (yaw angle), the effect of this aerodynamic yawing moment tends to increase the angle β further.

A clear illustration of the flow characteristics of standard production vehicles exposed to side winds is given by Sorgatz and Buchheim[5.7] and shown in Fig. 5.5. For small yaw angles, very high negative (suction) pressures occur at the leeward side of the vehicle's front end and the leeward A-pillar, whereas further downstream the leeward side exhibits low negative pressures only. For larger angles of yaw, the air flow separates at the leeward front fender corner and at the A-pillar, which results in smaller negative pressure peaks in these areas. The kink in the curve of the frontal side-force coefficient indicates the beginning of the transition to separated flow.

At the windward side of the front end, low positive pressure exists which

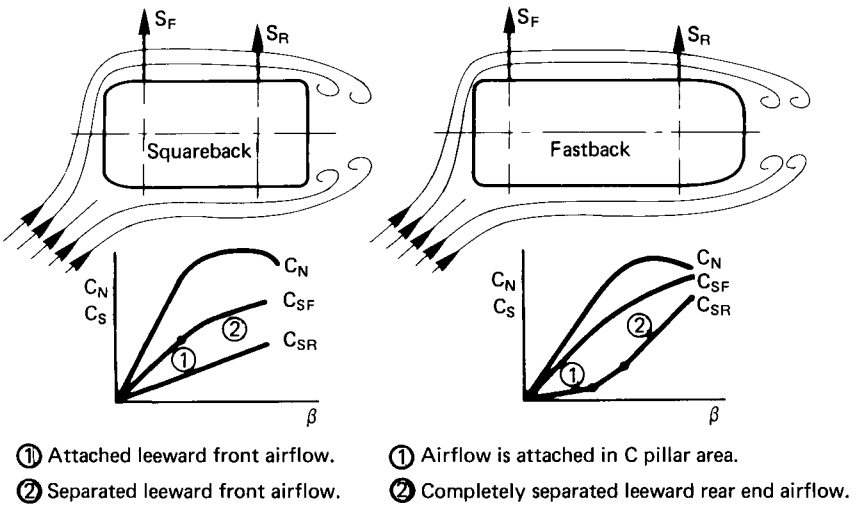

Figure 5.5 Airflow conditions and forces acting on the car exposed to side wind, after ref. 5.7

turns to low negative pressure further downstream. The magnitude and extent of the positive pressure region grow as yaw angle increases. For such yaw angles, vehicles exhibiting well-tapered and rounded rear ends and C-pillars exhibit a significant pressure increase at the leeward side at their rear ends and a corresponding pressure decrease at the windward side.

For further increased yaw angles this trend is reversed and it slowly diminishes until it disappears, due to a substantial change in the characteristics of separation at the rear end and vortex patterns at the C-pillars.

Fastback and notchback cars therefore show a different slope of the rear side-force coefficient from squareback vehicles. For small yaw angles, fastback vehicles show a slight slope of the rear side-force coefficient which changes to a steeper slope for larger yaw angles. At this stage the slope of the yawing moment coefficient becomes negative.

The question now arises of how the slope of the side-force coefficient or the yawing moment coefficient, respectively, can be influenced by contour changes.

From aerofoil aerodynamics it is known that an aerofoil section that is stalled, exhibiting separation on the upper side, has very low lift and a small pitching moment. When this principle is applied to a vehicle, it means that sharp edges on the front corners of the vehicle, although increasing vehicle drag, can reduce the side force and yawing moment on the vehicle.

The conflicting goals between designing for optimized drag and reduction of side-wind force and yawing moment are overcome by optimizing the vehicle front for separation-free flow for yaw angles between $-10° \leqslant \beta \leqslant +10°$, which is a region in which side winds cause relatively little concern. For larger yaw angles, where side winds cause more concern, separation of the airflow is permitted in order to reduce the yawing moment. The subsequent increase in drag can then be tolerated, because these larger yaw angles occur only briefly. The 'matching' for low

drag at small yaw angles and low yawing moments at higher yaw angles is to be seen in Fig. 5.6, after Hucho.[5.27] This condition is simplest to realize during the optimization of box vans—as illustrated by Hucho.[5.8]

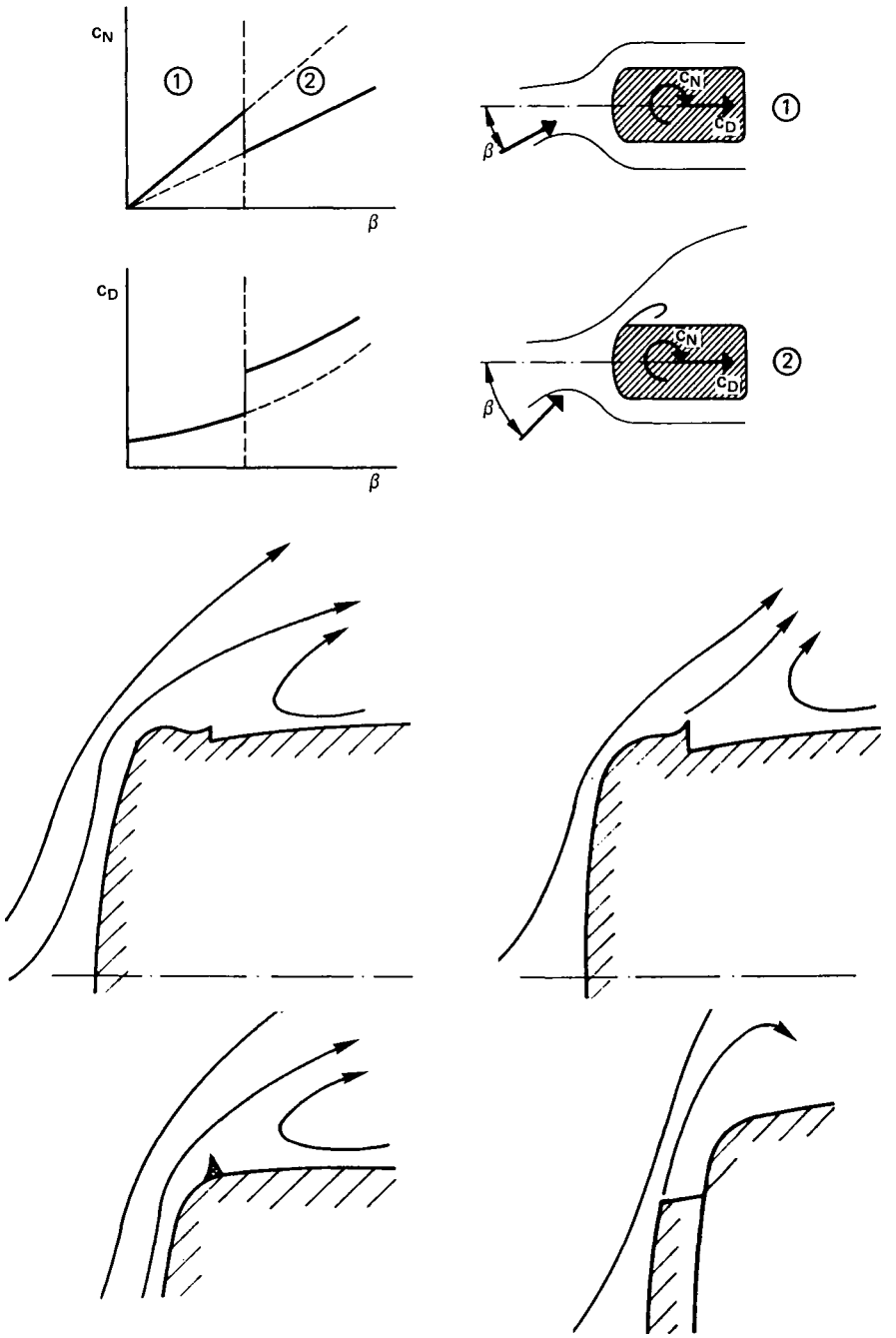

Figure 5.6 Reduction of yawing moment by controlled separation, after ref. 5.27

In vehicle dynamics, moments are usually related to a reference point at the centre of the wheelbase and centre of the track, at road level. With regard to side-wind sensitivity however, the yawing moment N_{SP} is referenced to the vehicle centre of gravity, around which the yawing motion occurs, see Fig. 5.7.

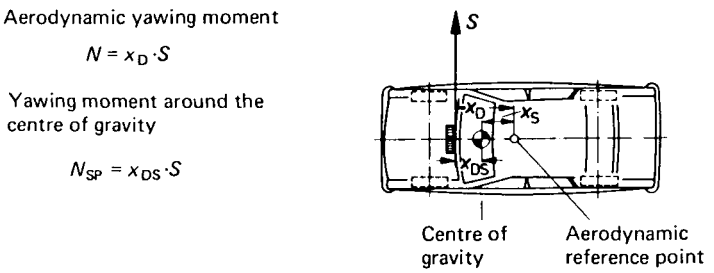

Figure 5.7 Definition of centre of pressure

The two reference points for yawing motion are only identical if the vehicle's weight is equally distributed on the front and rear axles. Increased rear axle loading increases the mechanically induced yawing moment and increased front axle loading reduces it, compared with the aerodynamic yawing moment. The latter can even result in a change of sign of the stability expression.

The possibilities for influencing aerodynamic forces and moments by modifying the vehicle shape are shown in Fig. 5.8 and further detailed in

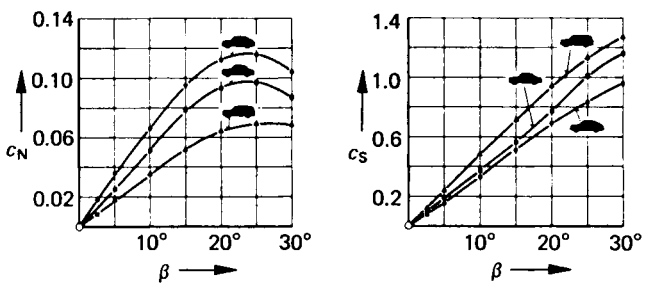

Figure 5.8 Yawing moment and side-force coefficients for a vehicle with different rear end shapes

Fig. 5.9. From Fig. 5.8 it can be seen that yawing moment and side-force coefficients are extremely dependent upon the vehicle rear end configuration. The smallest yawing moment and the largest side forces are found with the squareback configuration, whereas the fastback exhibits the smallest side force and the largest yawing moments. The notchback configuration exhibits intermediate values for both side forces and yawing moments. The evaluation of the effect of the above forces and moments on the sideways deviation of a vehicle from its desired direction is discussed in section 5.5.3.

The lift forces shown in Fig. 5.9 are of similar magnitude to drag. However, they only affect directional stability at speeds above roughly 100 km/h (62 mile/h) because at lower speeds they are small relative to vehicle weight and their 'unloading' effect on the tyres is small.

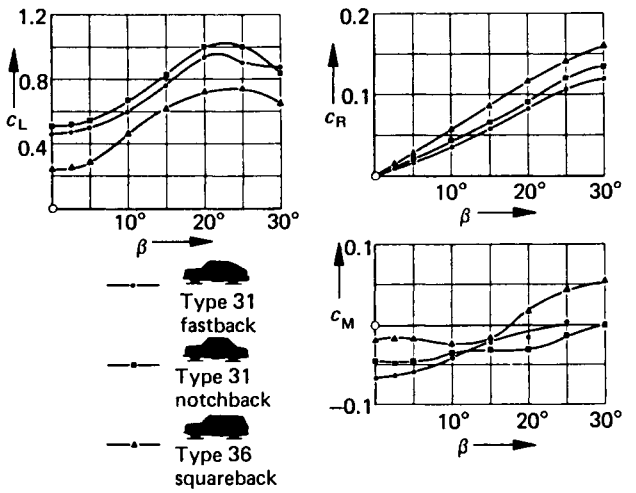

Figure 5.9 Lift and rolling and pitching moment coefficients for a vehicle with different rear end shapes

In the case of fast coupés or sports cars, lift must be reduced by modification of vehicle shape or addition of supplementary spoilers at the front and/or the rear of the vehicle. To increase maximum cornering speeds of racing cars, spoilers or wings provide negative lift, even at the cost of increased drag and therefore reduced top speed (see section 7.4.1).

5.2.4 Wind forces resulting from non-steady side winds

As mentioned in section 5.2.1, speed and direction of natural side wind vary from place to place. In addition to the side-wind forces and moments, which generally are measured under steady state conditions in a wind tunnel, further components must be considered, as indicated schematically in Fig. 5.10. The components can be split into three parts: constant,

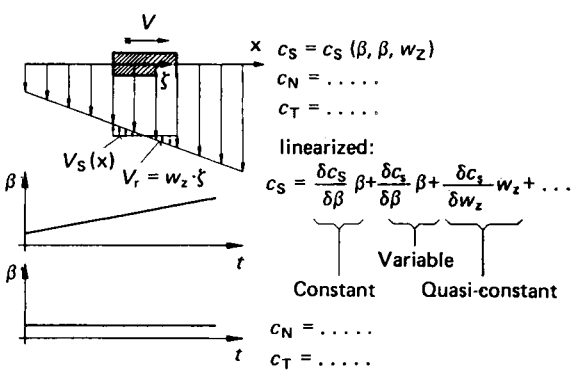

Figure 5.10 Linearized view of stationary airflow forces and moments for variable side-wind profiles

quasi-constant (turning motion) and variable. The last are to be expected in steep wind gradients where the normalized frequency is

$$\Omega = \frac{\omega l}{V} > 1$$

According to Reichard,[5.9] side-wind profiles vary relative to normal free airflow limits according to a cosine relationship. Hucho and Emmelmann[5.10] have, by application of the Slender Body Theory (see also Hummel[5.11] and Woolard[5.12]) calculated the development of yawing moments and side forces for such side-wind profiles. The results of these calculations are shown in Fig. 5.11.

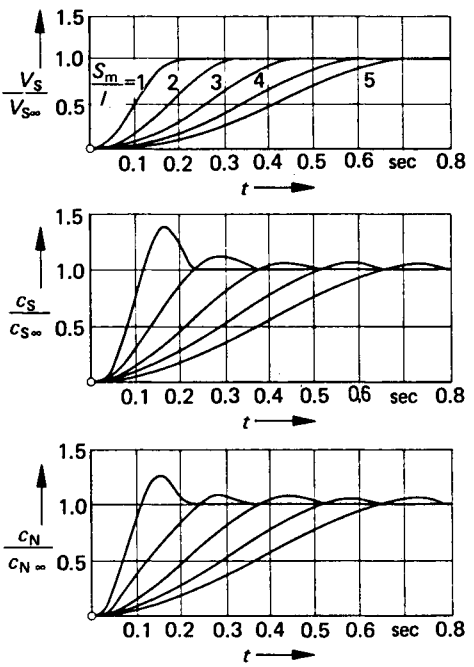

Figure 5.11 Computed variable side-force and yawing moment coefficients for different side-wind profiles, after ref. 5.10

In the upper part of the figure, the applied wind profile can be seen in plan view. V_s is the local side-wind speed, $V_{s\infty}$ the constant speed of side wind following the transition. The parameter is based upon vehicle length l, relative to the transition length S_M, of the wind profile from wind speed $V_s = 0$ up to the attainment of full wind speed $V_{s\infty}$. From this it can be seen that, as a result of steep wind profiles, the variable portion leads clearly to an 'overshoot' situation, in terms of side force and yawing moments, during which these forces and moments approach those resulting from a flat wind profile. Measurements by Beauvais[5.13] and Muto[5.14] confirm this overshoot phenomenon, which results from spatially varying side winds. Measurements conducted by Emmelmann[5.25] using a model side-wind simulator (Fig. 5.12) showed that, as expected, the theory outlined in ref.

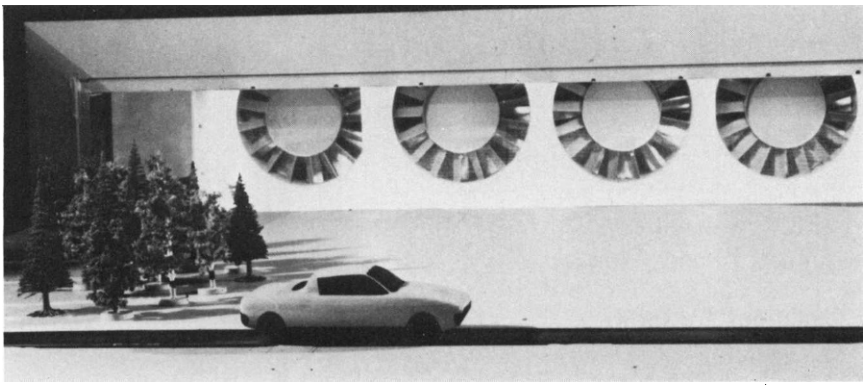

Figure 5.12 Model side-wind track for measurement of side forces and yawing moments, after ref. 5.25

5.10 only correlates with experiment in the case of vehicle bodies having what could be described as slender front ends.

5.3 Real side-wind problems

5.3.1 Traffic routes, wind protection

Traffic routes are normally established without regard for side-wind danger. Underpasses, embankments and bridges are particularly exposed. In contrast to the statement made in section 5.2.1, where it was said that lower wind speeds are normally experienced at vehicle level than at 10 to 15 metres above ground level, Fig. 5.13 shows that buildings and

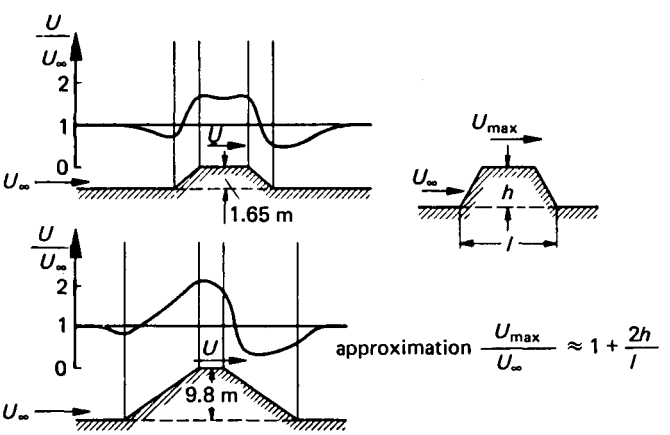

Figure 5.13 Increased speed on embankments under side-wind conditions, after ref. 5.2

man-made features, i.e. embankments, can increase wind speeds above the speed of ambient wind. Gaps in bushes and tree spacing can cause a jet effect which raises local wind speeds above the normal wind speed in open spaces. These findings were taken from the work by Bitzl[5.2] and are illustrated in Figs 5.13 and 5.14.

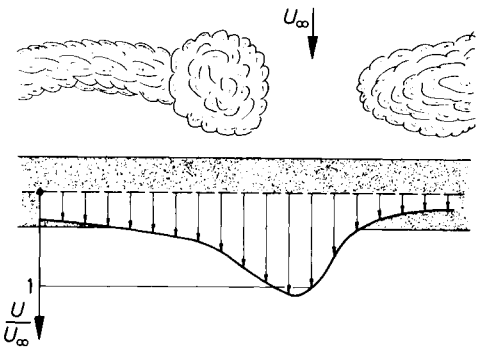

Figure 5.14 Side-wind jet effect from a gap in roadside bushes, after ref. 5.2

Impermeable hedges and wooden protective fences are equally effective in reducing wind speed, according to the Heppenheimer model (Fig. 5.15, from Blenk and Trienes[5.15]). However, wind speed can be accelerated by roadside trees, such as poplars, due to the displacement effect of the tree tops.

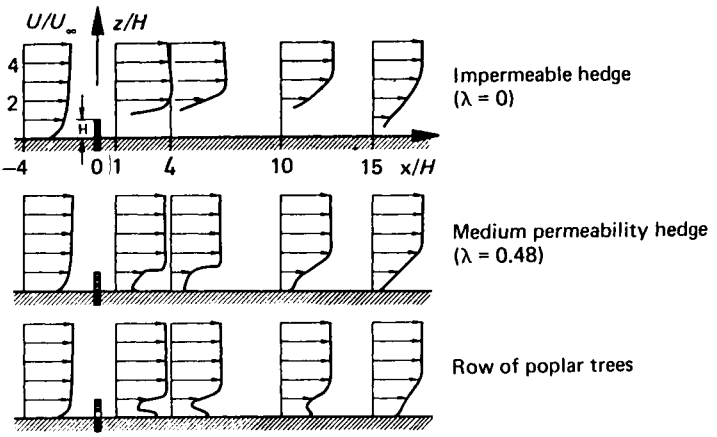

Figure 5.15 Wind profiles behind various types of hedges (model tests), after ref. 5.15

Good wind protection is offered on roads which pass through country areas (Fig. 5.16). Results to confirm this were obtained from tests conducted by the author on a 1:16 scale countryside model in the full-scale wind tunnel of Volkswagen AG.

5.3.2 Natural and artificial side-wind gusts

It was stated above that the turbulence level of natural wind is of the order of unity: $Tu \approx 1$. Thus when the side wind has the velocity V, the speed can suddenly increase to $2V$ or drop to zero. The effect of natural wind squalling seems to be the same regardless of whether the cause is building development or vegetation (bushes, etc.). Whereas the constant side-wind conditions indicated in Fig. 5.13 can be compensated for by a constant

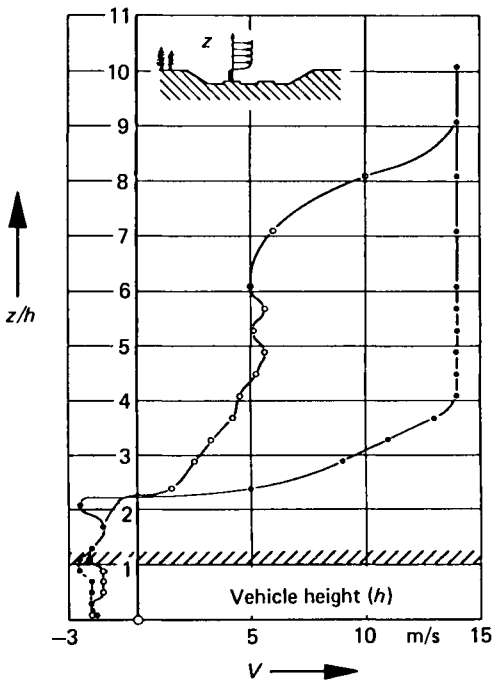

Figure 5.16 Wind speed distribution through a section of countryside (scale 1:16)
• without trees
○ with trees

steering angle, the side-wind case shown in Fig. 5.14 cannot be anticipated and calls for sudden correction. It is therefore more dangerous.

The same applies to driving between bridge abutments under side-wind conditions. Initially the vehicle moves in a constant side-wind area (Fig. 5.17) with an appropriate constant steering angle towards the wind. It then comes into the sheltered area adjacent to the bridge abutment, and the driver must then steer to the left in order to avoid driving off the right-hand side of the road. With this new steering angle the vehicle is then again exposed to side wind from the right, which leads to a violent reaction by the driver.

Every driver is familiar with the problem of overtaking a truck under side-wind conditions. Due to the relative velocities of the two vehicles, the overtaking speed is small compared to the driving speed and a small wind frequency results. Non-steady wind effects are therefore not normally expected. It is therefore possible to simulate and measure this overtaking situation using constant side wind in the wind tunnel.

Figure 5.18, after Emmelmann,[5.16] shows the effect on the vehicle yawing moment when it overtakes a container truck. Large yawing moments are found, endangering the driver/vehicle system, when the vehicle emerges from the sheltered side of the container truck, where it enters the displaced airflow field of the truck. This field exhibits increased airflow speed, relative to the normal side-wind speed, coupled with larger deflection angles. The amplitude Δc_N is dependent on the lateral distance

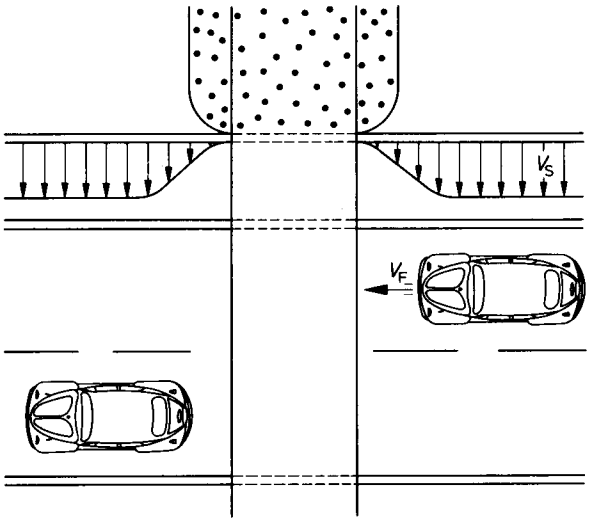

Figure 5.17 Schematic showing side-wind speed distribution in the vicinity of bridge abutments

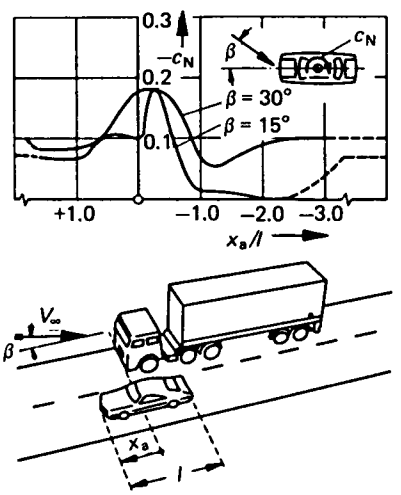

Figure 5.18 Yawing moment change during the overtaking of a container truck by a car, after ref. 5.16

between the two vehicles during the overtaking manoeuvre. In principle the effect is the same for every shape of vehicle. However, the magnitude of yawing moment change can be reduced by rounding the front corners of the truck.

5.4 Vehicle dynamics under side wind

No general definition exists for the side-wind sensitivity of vehicles. In the majority of the many studies into this problem the effect of side winds on

vehicles has been established either from test results or with the help of computer models (Fiala,[5.17,5.18] Gnadler,[5.19,5.20] Mitschke,[5.21,5.22] Sorgatz[5.23]).

In order to represent the side-wind sensitivity phenomenon completely, the driver must also be taken into consideration. The relationship between the driver and the vehicle, as shown in Fig. 5.19, must be fully understood.

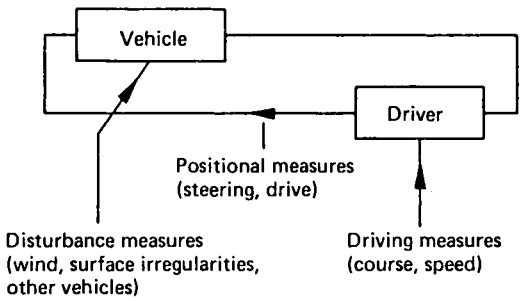

Figure 5.19 Driver/vehicle control system

The necessary investigation is however complicated by the fact that the driver is an adaptive controller; that is to say, he or she adapts to the characteristics of the vehicle being driven. There are so many unknowns with regard to driver adaptability that the driver/vehicle system cannot yet be fully explained theoretically.

Various assumptions concerning the behaviour of the driver have been made for the purpose of the various test methods and computer models (see Niemann[5.24]); i.e. driver behaviour is defined by a number of different statements—each case then being investigated to establish the manner in which the vehicle reacts under the influence of side-wind disturbance.

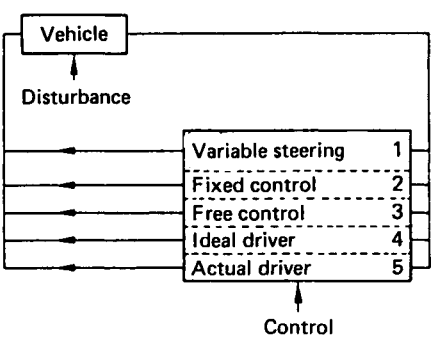

Figure 5.20 Possible representations of the driver/vehicle system

Figure 5.20 shows the various possibilities for consideration, whereby the vehicle can either be under 'fixed control' by the steering wheel being held firm, or under 'free control' by allowing the steering wheel to turn freely. Measurements have been conducted by Fiala[5.17] to evaluate cases 2, 3 and 5.

The corresponding two diagrams (see Fig. 5.21) indicate the change in angular direction γ and lateral deviation y_G of the centre of gravity of the vehicle as a result of the use of a hot water rocket mounted on the vehicle,

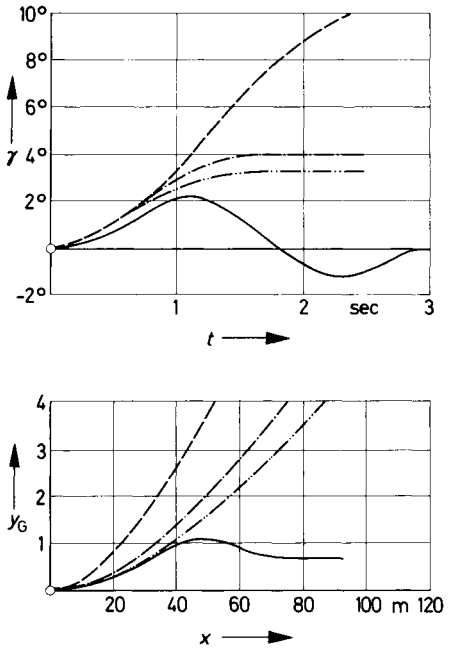

Figure 5.21 Slip angle and lateral deviation for various driver reactions.
——— driver steers against deviation
—··— steering wheel held firm (fixed control)
—·— steering wheel allowed to move freely
-------- driver steers against deviation, and brakes

which simulates a side wind. These variables are plotted against time t. From tests it was discovered that the real driver, case 5, began to make steering corrections after a reaction time of approximately 0.2 seconds. Due to steering play, elasticity and the variable nature of the side forces it was however 0.8 seconds before the vehicle 'noticed' any effect from the driver's reaction.

Until this time, the yawing rate and resultant lateral deviation are similar for all cases investigated. For the specific case however, where a vehicle is under fixed control and its reaction to side-wind squalls is analysed, reasonable results are obtained by evaluating lateral deviation y_G after a time lapse of 0.8 seconds. In the following section, calculations for the fixed control case are analysed with the aim of evaluating the effect of wind forces on lateral deviation. Representative test methods are described in section 12.4.2.

5.5 The effect of aerodynamic forces on lateral deviation

5.5.1 Reduction of the number of parameters

The lateral deviation of a vehicle from its intended path, under fixed control conditions, is dependent upon a number of factors additional to the actual wind profile that is causing the disturbance. These factors include

the weight G of the vehicle, the moment of inertia I_{zz} of the vehicle about the vertical axis through the centre of gravity of the vehicle, the load distribution between front and rear axles and the design of the chassis. In this last factor the influence of the tyres, steering elasticity and type of suspension are reflected.

The extent of the disturbance is influenced by the aerodynamic side force and the associated yawing moment, and also by lift, roll and pitching moments. Because parameter tests in a side-wind simulator are very time-consuming it is worthwhile to use an accurate computer model. The data that follows have been calculated using the previously mentioned computer model by Sorgatz.[5.23]

This computer program allows for a full description of the vehicle to be entered in 23 degrees of freedom using a large amount of input data. In order to evaluate standard vehicles which are perhaps only modified in minor chassis characteristics, it is possible to use standard data so that observation can be concentrated only on the following important side-wind deviation parameters:

- Vehicle weight G
- Weight distribution G_f/G_r (centre of gravity position)
- Moment of interia I_{zz} about a vertical axis through the centre of gravity
- Yawing moment N
- Side force S

As Fig. 5.22 shows, good correlation exists between vehicle weight G and the moment of inertia I_{zz} about a vertical axis through the centre of gravity,

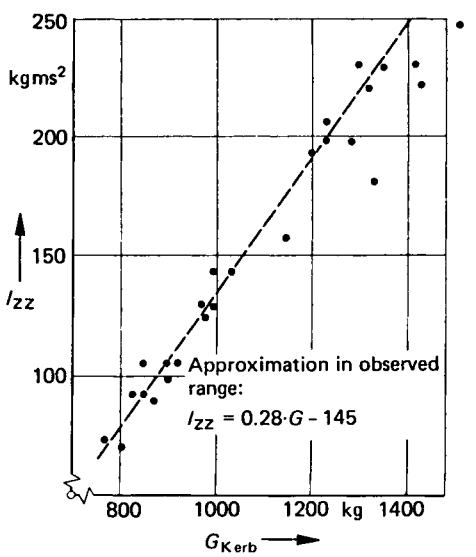

Figure 5.22 Comparison of vehicle weight and moment of inertia around the vertical axis through the centre of gravity

for vehicle weight between 700 and 1500 kg. In this region the relationship is approximately a linear function.

$$I_{zz} = 0.28G - 145\,\mathrm{kg\,m\,s^2} \tag{5.1}$$

A yawing moment exists around the zz axis, which passes vertically through the vehicle's centre of gravity. It results from the aerodynamic forces that act at the aerodynamic reference point adjacent to the centre of gravity of the vehicle (see Fig. 5.7):

$$N_{SP} = x_s S \tag{5.2}$$

When one divides this yawing moment by the side force, an aerodynamic lever arm length x_{DS} is established (the distance from the so-called centre of pressure to the centre of gravity).

$$x_{DS} = \frac{N_{SP}}{S} = \frac{N}{S} - x_S = x_D - x_S \tag{5.3}$$

This expression 'centre of pressure' assumes that the yawing moment was the result of side force only.

In reality the yawing moment is generated by the side force and the drag (tangential force), because the latter is acting in the same plane as the side force and, of course, for yawed flow the tangential force will act with a lever arm from the aerodynamic reference point. Therefore the expression 'centre of pressure', taken from aerofoil aerodynamics where the influence of drag and its lever effect compared with the influence of the lift is negligible, is misleading in the case of automobiles.

The following evaluation of the effect of aerodynamic coefficients and the weight parameters on lateral deviation requires the choice of a wind profile along the virtual test track. The chosen profile, shown in Fig. 5.23,

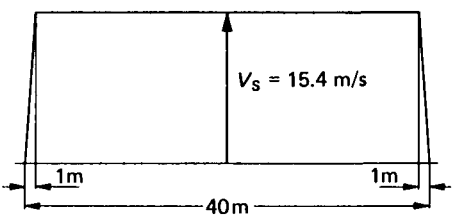

Figure 5.23 Artificial wind profile

is trapezoidal, closely resembling the profile of the Volkswagen AG outdoor side-wind facility. With a driving speed of $V = 26.7$ m/s (60 mile/h, according to RSV Specifications, RSV = Research Safety Vehicle) a yaw angle of $\beta = 30°$ results. After time $t = 0.8$ s the vehicle is still exposed to constant side wind along its complete length.

5.5.2 Equation for evaluation of the influence of side force, weight and aerodynamic lever arm length

The previously mentioned computer model by Sorgatz was used to analyse two completely different vehicles by varying the side force, yawing moment and centre of gravity positions, with, as previously described, the remainder of the parameters all standardized. One vehicle was front wheel drive weighing 996 kg, the other was equipped with a rear mounted engine and rear wheel drive, and weighed 1506 kg.

Following the calculations with these vehicles, a regression analysis was conducted for the computed lateral deviations, with a view to establishing

the influence of the parameters of weight, aerodynamic lever arm length x_{DS} and side force, the latter substituted by the product $c_S A$.

The side force coefficient c_S at the yaw angle $\beta = 30°$ was chosen to represent lateral deviation caused by the side-wind profile; this coefficient was then called c_{S30}. The following equation resulted:

$$y_G = \left[\frac{1}{G}(k_1 + k_2 x_{DS}) + k_3 x_{DS} + k_4\right] c_{S30} A + \\ + \frac{1}{G}(k_5 + k_6 x_{DS}) + k_7 x_{DS} + k_8 \qquad (5.4)$$

where G is in kg, x_{DS} is in m and A is in m^2, and the following constants for the particular side-wind case after time $t = 0.8$ s are valid:

k_1 =	58.820	k_5 =	182.350
k_2 =	135.290	k_6 =	−279.410
k_3 =	0.028	k_7 =	0.215
k_4 =	0.014	k_8 =	− 0.095

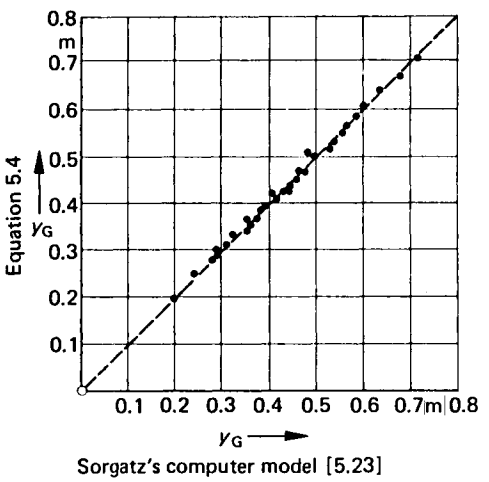

Figure 5.24 Comparison of the results of Eqn 5.4 and those of the original calculations by Sorgatz[5.23]

As can be seen in Fig. 5.24, good correlation exists between the results of Eqn 5.4 and the deviation magnitudes calculated using the complete model of Sorgatz. Eqn 5.4 can therefore be used to calculate the lateral deviation of production vehicles under side wind.

5.5.3 Calculation of lateral deviation for production vehicles

Equation 5.4 was used to calculate lateral deviation for a range of 30 vehicles. Figure 5.25 shows plots of x_{DS} versus respective side force coefficient $c_{S30} F$. From this plot a trend can be seen, indicating that for vehicles with small side-force coefficients the aerodynamic lever arm is longer than for vehicles with large side forces.

The lateral deviations y_G, calculated using Eqn 5.4 normalized to the

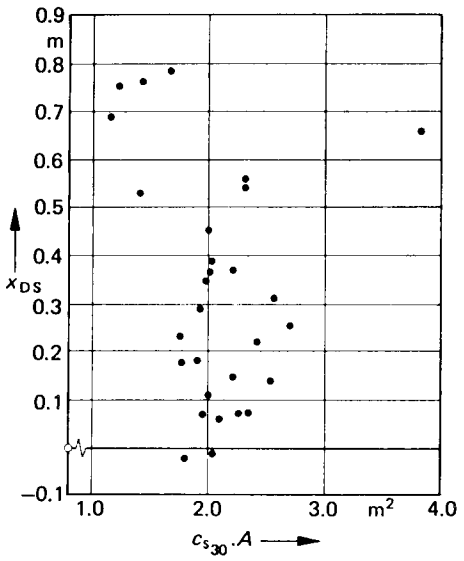

Figure 5.25 Side-force coefficients and centre of pressure distance for actual vehicles

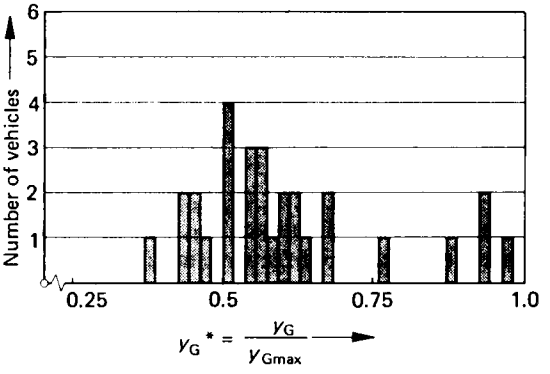

Figure 5.26 Frequency distribution of lateral deviation, computed using Eqn 5.4, for 30 production vehicles

largest lateral deviation y_{Gmax} of the vehicles 'tested', are shown in Fig. 5.26 as a frequency distribution. The arithmetical mean value is $y_G^* = 0.63$, with only 30 per cent of the vehicles tested exhibiting deviation larger than this mean, and approximately 50 per cent of the vehicles deviating less than $y_G^* = 0.57$.

5.6 Safety limit

The limit above which side-wind sensitivity becomes dangerous rather than just uncomfortable is not only dependent on the frequency distribution of side-wind deviation. With the help of an assumption, an attempt will be made to measure and specify the limit of safety.

A dangerously large side-wind deviation can be specified as one that causes the vehicle to deviate to the side of the driving lane. With a driving

lane width of 3.75 m (German Autobahn; USA highway is approximately 3.66 m) and a vehicle width of approximately 1.70 m, only about one metre of road width is available for course deviation from the optimum middle-of-the-lane driving position; see Fig. 5.27.

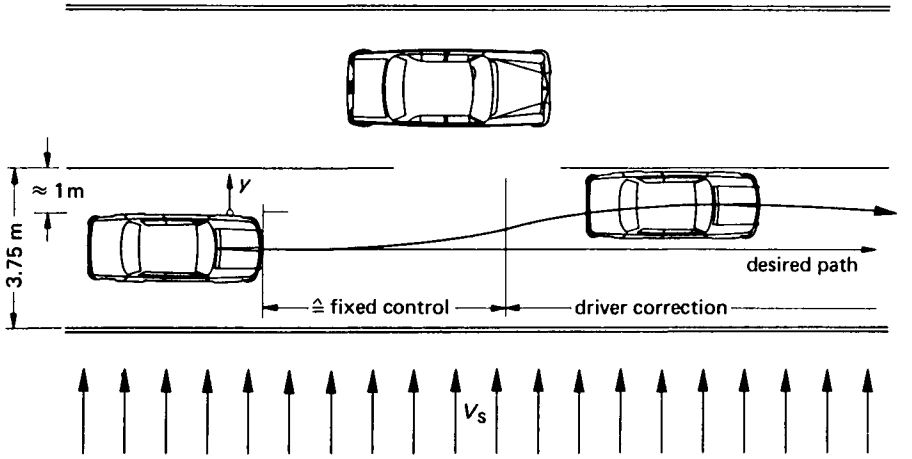

Figure 5.27 Vehicle course as a result of side wind (schematic)

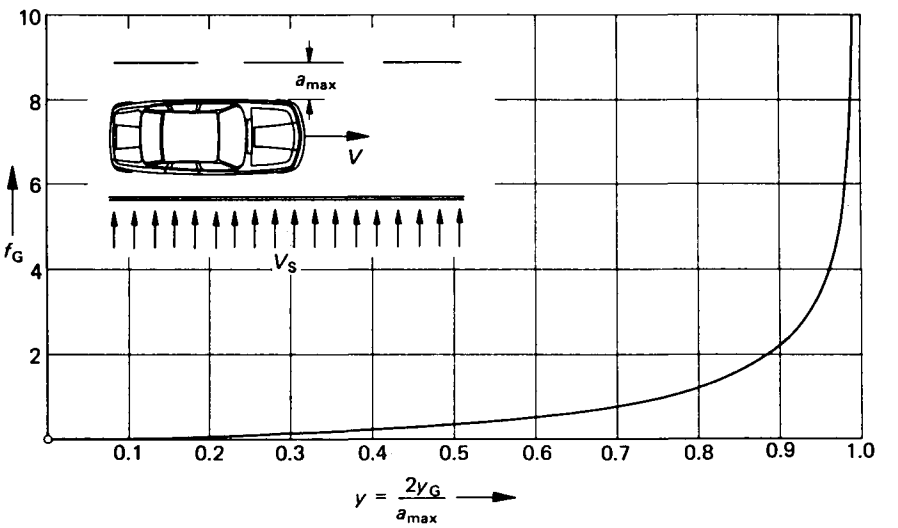

Figure 5.28 Danger level with increasing proximity to the side of the driving lane

As an initial assumption, one can say that a vehicle will deviate from its desired course by approximately twice the deviation y_G, which occurs while the vehicle is under fixed control during the first 0.8 seconds after wind changes begin (see Fig. 5.21) and before driver reaction 'recovers' the vehicle.

Assuming that the original course is in the middle of the driving lane, the level of danger increases slowly as the vehicle deviates from this course and

is not significant until the vehicle approaches the side of the lane—when the level of danger increases rapidly. This situation can be represented by the following formula (see Fig. 5.28):

$$f_G = \sqrt{\left(\frac{1}{1 - Y}\right)} - 1 \tag{5.6}$$

where

$$Y = \frac{2y_G}{a_{max}} \tag{5.7}$$

Under the assumed distribution of level of danger (Eqn 5.6), the danger can be seen to increase rapidly from $Y = 0.9$. If this were defined as the danger limit, it would mean that for the example illustrated in Fig. 5.27 ($a_{max} = 1$ m) a maximum allowable deviation of $y_G = 0.45$ is tolerable; i.e. minimum safe driving distance from the side of the lane is 0.1 m.

5.7 Outlook

The side-wind sensitivity of motor vehicles represents a disturbance to the vehicle/driver system which can vary from being merely a loss of comfort to a dangerous vehicle characteristic. Whereas the vehicle is theoretically relatively easy to describe, the driver can only be simulated by an idealized model that does not have the adaptive qualities of an actual driver. Driver simulation is an area which must therefore be investigated in the future. Attachments on this theme are presented by Wallentowitz,[5.26] who applied a frequency-dependent characteristic.

Until now, vehicle development has had to rely on simple evaluation methods; such a method has been described in this section.

5.8 Notation

A	reference area
I_{zz}	moment of inertia about vertical axis
N	yawing moment
S	side force
Tu	degree of turbulence
U	wind speed
V	driving speed
V_S	side-wind speed
Y	relative lateral deviation, Eqn 5.7
c_L	lift coefficient
c_N	yawing moment coefficient
c_M	pitching moment coefficient
c_R	rolling moment coefficient
c_S	side force coefficient
c_{S30}	side force coefficient at $\beta = 30°$
c_T	tangential force coefficient

f_G degree of danger, Eqn 5.6
l length of vehicle
q dynamic pressure
x_D centre of pressure distance
x_{DS} distance between centre of pressure and centre of gravity (aerodynamic lever arm length)
x_S centre of gravity distance
y_G lateral deviation
β yaw angle
γ slip angle